NEOPLASIA
www.neoplasia.com

Volume 11 Number 6 June 2009 pp. 518–528 518

Urokinase-Type Plasminogen Activator Receptor Transcriptionally Controlled Adenoviruses Eradicate Pancreatic Tumors and Liver Metastasis in Mouse Models[1,2]

Meritxell Huch*,†, Alena Gros‡, Anabel José*,†, Juan Ramon González§,¶,#, Ramon Alemany‡ and Cristina Fillat*,†

*Programa Gens i Malaltia. Centre de Regulació Genòmica-CRG, UPF, Parc de Recerca Biomèdica de Barcelona-PRBB, Barcelona, Spain; †Centro de Investigación Biomédica en Red de Enfermedades Raras (CIBERER), Barcelona, Spain; ‡Laboratori de Recerca Translacional. IDIBELL-Institut Català d'Oncologia, Barcelona, Spain; §Centre de Recerca en Epidemiologia Ambiental (CREAL), Barcelona, Spain; ¶Institut Municipal d'Investigació Mèdica (IMIM-Hospital del Mar), Barcelona, Spain; #Centro de Investigación Biomédica en Red de Epidemiologia y Salud Pública (CIBERESP), Barcelona, Spain

Abstract

Treatment options for pancreatic cancer have shown limited success mainly owing to poor selectivity for pancreatic tumor tissue and to a lack of activity in the tumor. In this study, we describe the ability of the urokinase-type plasminogen activator receptor (uPAR) promoter to efficiently and selectively target pancreatic tumors and metastases, which enables the successful management of pancreatic cancer. We have generated a replication-defective reporter adenovirus, AduPARLuc, and a conditionally replicating adenovirus, AduPARE1A, and we have studied the selectivity and antitumoral efficacy in pancreatic tumors and metastases. Toxicity was studied on intravascular delivery. We demonstrate that the uPAR promoter is highly active in pancreatic tumors but very weak in normal tissues. Tumor specificity is evidenced by a 100-fold increase in the tumor-to-liver ratio and by selective targeting of liver metastases ($P < .001$). Importantly, the AduPARE1A maintains the oncolytic activity of the wild-type virus, with reduced toxicity, and exhibits significant antitumoral activity (25% tumor eradication) and prolonged survival in pancreatic xenograft models ($P < .0001$). Furthermore, upon intravascular delivery, we demonstrate complete eradication of liver metastasis in 33% of mice, improving median survival ($P = 5.43 \times 10^{-5}$). The antitumoral selective activity of AduPARE1A shows the potential of uPAR promoter–based therapies in pancreatic cancer treatment.

Neoplasia (2009) 11, 518–528

Introduction

Pancreatic cancer is one of the most aggressive and devastating human malignancies in developed countries. Overall survival rate is less than 4%, with almost all patients dying within the first year after diagnosis as a result of the rapid spreading of the tumor or metastatic dissemination [1].

Up to now, pancreatic cancer treatment has mainly been palliative because of the ineffectiveness of current treatments [1]. Despite the great efforts made to improve therapy, even the very latest therapeutic approaches assayed, such as the combination of gemcitabine with epidermal growth factor receptor–targeting agents, have shown only partial improvement on patients survival [2]. Thus, there is an urgent need for more intensive research seeking ways to treat this devastating disease.

Address all correspondence to: Cristina Fillat, Centre de Regulació Genòmica-CRG, Parc de Recerca Biomèdica de Barcelona-PRBB, Dr. Aiguader, 88, 08003-Barcelona, Spain. E-mail: cristina.fillat@crg.es

[1]This work was supported by the Spanish Ministry of Education and Science, BIO2005-08682-C03-02/01 and received partial support from the Generalitat de Catalunya SGR0500008 and European Commission Theradpox contract LSHB-CT-2005-018700. M. Huch was supported by a fellowship (BEFI) granted by the Instituto de Salud Carlos III, Spain.

[2]This article refers to supplementary materials, which are designated by Figures W1 to W4 and are available online at www.neoplasia.com.

Received 30 December 2008; Revised 4 March 2009; Accepted 5 March 2009

DOI 10.1593/neo.81674

The most important challenge to the development of a safe and effective treatment of pancreatic cancer is the identification of a selective therapeutic agent capable of potent activity both in primary tumors and in tumor metastases with low toxicity when administered systemically. Recently, oncolytic adenovirus therapy, based on restricting viral replication to cancer cells, has emerged as a promising candidate for cancer therapy [3]. The phase 1/2 clinical trials assaying the oncolytic efficacy of ONYX-015 have shown no major toxicity on intravascular infusion [4] but only partial therapeutic benefit when administered intratumorally to pancreatic tumors [5]. Therefore, the remaining issue is still to obtain a virus with sufficient activity and selectivity to the tumor tissue. To achieve tumor-selectivity, several tumor-specific promoters (TSPs) have been assayed for pancreatic cancer. However, they have shown lower activity in comparison to ubiquitously active promoters such as the cytomegalovirus (CMV) [6,7], unless the cholecystokinin type A receptor promoter when engineered with a VP_{16}-GAL4-WPRE integrated systemic amplifier [8]. When used in the context of conditionally replicative adenovirus, although significant responses have been reported for candidate TSP when administered intratumorally, limited antitumor activity has been observed on established xenografts upon intrasvascular delivery, and no studies have been performed on metastatic models [9–11].

The urokinase-type plasminogen activator receptor (uPAR) is a glycosylphosphatydilinositol-anchored protein that binds with high affinity uPA, pro-uPA, amino terminal fragments of urokinase, and other cell receptors. The uPAR has an active role in cancer because it regulates cell migration, adhesion, metastasis, and tumor growth [12]. In pancreatic cancer and in tumor metastasis, uPAR has been found to be overexpressed [13,14].

Several reports have shown that the down-regulation of uPAR expression with uPAR antagonists, small interfering RNA, or antisense genes prevents tumor growth, invasion, and metastasis [15]. Bauer et al. [16] also described how combining gemcitabine and a monoclonal antibody against uPAR reduces pancreatic cancer invasion in orthotopic tumors.

In the present study, we have also targeted uPAR expression in pancreatic cancer but using a completely different approach. We have validated the uPAR promoter to selectively target adenovirus gene expression and replication to primary pancreatic tumors and metastases. To our knowledge, for the first time, the present study demonstrates that upon intravascular injection, uPAR promoter activity is very weak in normal tissues, whereas in pancreatic tumor models and liver metastases, uPAR promoter activity is similar to that of the CMV promoter. Importantly, our results show that the conditionally replicative adenovirus AduPARE1A, in which replication is controlled by the human uPAR promoter, eradicates pancreatic tumors and tumor metastasis.

Materials and Methods

Plasmid Constructs

A 450-bp fragment encompassing the –402/+48 region of the uPAR promoter was excised from pCAT-Basic-uPAR(C2) [17] and subcloned into a pAdTrack to generate pAdTrackuPARp. The cDNA from luciferase was excised from the pGL3-Enhancer (Promega, Madison, WI) plasmid and subcloned into the pAdTrackuPARp to generate pAdTrackuPARLuc.

Cell Lines

The human pancreatic adenocarcinoma cell lines PANC-1, BxPC-3, RWP1, NP-31, NP-9, and NP-18 were obtained and cultured as previously described [18]. A549 human lung cancer cells, MCF-7 human breast cancer cells, NIH3T3 murine fibroblasts, IMR-90 human lung fibroblasts, and HEK293 were obtained from the American Type Culture Collection (ATCC, Rockville, MD) and maintained as already described [18,19]. U2 OS human osteosarcoma cells were obtained from European Collection of Cell Cultures (Wiltshire, United Kingdom) and were cultured following the manufacturer's description. Human pancreatic ductal epithelial (HPDE) cells were kindly provided by Dr. F.X. Real (IMIM, Barcelona, Spain) and cultured and maintained as reported [20]. Luciferase-expressing cells PANC-1-Luc were established by transducing the parental cells with luciferase recombinant retrovirus. Briefly, pLHCLuc retroviral vector was transfected by the calcium/phosphate–DNA precipitation method into the amphotropic packaging cell line Phoenix Ampho (ATCC, Rockville, MD), and 48 hours after transfection, viral supernatant was collected, passed through 0.45-nm filters, and used for transduction. Twenty-four hours later, cells were selected in 0.2 mg/ml hygromycin. Cells were cloned and tested for luciferase expression.

Transfection

Transient transfections were performed in NIH3T3, HPDE, and RWP1 cells, 24 hours after seeding, with SuperFect Transfection Reagent (Qiagen, Hilden, Germany) according to the manufacturer's protocol using 3 μg of plasmid DNA. Three micrograms of pCMV β-galactosidase plasmid was cotransfected to normalize for transfection efficiency.

Adenoviruses

Replication-defective adenoviruses AdCMVGFPLuc and AduPARLuc express the firefly luciferase gene under the control of CMV or uPAR promoter, respectively. AdCMVGFPLuc has already been described [21]. The AduPARLuc was generated by the homologous recombination of the pAdTrackuPARLuc and the adenoviral genome following a standard protocol.

The oncolytic AduPARE1A was constructed by inserting the uPAR promoter (450-bp fragment) upstream of an *E1a* adenoviral gene in which the E1a translation start site was replaced by the Kozak sequence. The human DM-1 insulator was cloned upstream the uPAR promoter [9,22]. All cassettes were cloned in a left-to-right orientation. The wild-type virus, Adwt, was obtained from the ATCC (Manassas, VA). Replication-defective AdV has already been described [23]. Replication-defective viruses and Adwt were propagated in HEK293 cells, and the oncolytic AduPARE1A virus was amplified in RWP1 cells. All viruses were purified by standard cesium chloride banding. The physical particle concentration (vp/ml) was determined by optical density reading (OD_{250}), and the plaque-forming units (pfu/ml) were determined by tissue culture infectious $dose_{50}$ titration on HEK293 cells. AdCMVGFPLuc and AduPARLuc presented an equal ratio of vp and pfu.

Tumor Growth Studies

BxPC-3 cells (2.5×10^6) were injected subcutaneously (SC) into each posterior flank of BALB/c nude mice (Charles River France, Lyon, France). Tumors were measured three times a week, and volumes were calculated according to the formula V (mm^3) = larger diameter (mm) × smaller diameter 2 (mm^2) / 2. Treatment was initiated when tumors achieved a mean volume of 50 mm^3. All animal procedures met the guidelines of European Community Directive 86/609/EEC and were approved by the local ethical committee.

Bioluminescence Assay and Quantification

Animals were anesthetized and the substrate D-Firefly-Luciferin (Xenogen, Alameda, CA) was administered intraperitoneally (32 mg/kg). Luciferase activity was visualized and quantified using an *in vivo* bioluminescent system (IVIS50; Xenogen) and Living Image 2.20.1 Software overlay on Igor Pro4.06A software (Wavematrics, Seattle, WA) as described [23]. Luciferase activity was quantified from non-saturated images, measuring the total amount of emitted light recorded by the CCD camera.

Immunohistochemistry and Stereological Analysis

Five-micrometer sections were deparaffinized, rehydrated, and treated with 10 mM citrate buffer (pH 6.0) for antigen retrieval. Sections were then incubated overnight with a rabbit anti–luciferase polyclonal antibody (1:500; Sigma, Poole, United Kingdom). Bound antibodies were detected with Universal LSAB+ (DAKO Diagnostics, Denmark). Sections were counterstained with Mayer's hematoxylin. All sections were examined on a Leica DMR microscope (Leica, Madrid, Spain).

A physical dissector method was used to estimate the luciferase-positive cells per squared millimeter in both the liver and tumoral areas, with the aid of a CAST-GRID software package (Olympus, Denmark) adapted to an Olympus BX51 microscope. At least three independent, nonsequential, randomly selected liver sections or three tumor sections were counted from each animal. A mean of 25 dissector probes (dis), of 17,110 μm^2 (Sdis), were analyzed per liver area with a ×10 lens. A mean of 160 dissector probes of 57,043 μm^2 was analyzed per tumoral area with a ×40 lens. The total final surface area analyzed was similar for each of the different viral groups. The number of cells per squared millimeter was calculated according to the formula: [N (cells/mm^2) = N cells/N dis × Sdis].

Liver Toxicity Studies and Determination of the Adenoviral DNA Content in Liver

For liver toxicity studies, 6- to 8-week-old immunocompetent BALB/c male mice received a single administration of the corresponding virus at a final dose of 2×10^{10} vp (AduPARLuc) or 5×10^{10} vp (AduPARE1A) in a final volume of 0.2 ml injected into the tail vein. Body weight, morbidity, and moribundity were monitored daily. Blood samples were collected by intracardiac puncture under anesthesia. Serum aspartate aminotransferase (AST) and total bilirubin (BLT) were determined on an Olympus AU400 Analyzer. Subsequently, the animals were killed, and liver portions were either frozen for luciferase or viral DNA determination or fixed and embedded in paraffin for hematoxylin and eosin staining or frozen in OCT (Akura Finetek, Zoeterwoude, the Netherlands) for E1A immunodetection.

E1a immunodetection was performed by incubating the OCT-embedded liver sections with a primary polyclonal antibody anti–adenovirus-2 E1a (clone 13 S-5; Santa Cruz Biotechnology, Heidelberg, Germany). AlexaFluor 488–labeled goat anti–rabbit antibody (Molecular Probes, Eugene, OR) was used as a secondary antibody. The nuclei were counterstained with 5 μg/ml bis-benzimide (Hoechst 33342; Sigma) and visualized under a fluorescent microscope (Observer/Z1; Zeiss, Barcelona, Spain). The fluorescent images were captured using a digital camera (AxioCamMRm; Zeiss).

When stated, DNA was obtained from frozen liver tissue by incubating in a buffer containing 0.2 mg/ml RNaseA and 0.1 mg/ml protease overnight at 55°C. The liver adenoviral DNA content was determined with real-time polymerase chain reaction (PCR; 100 ng of DNA) and SYBER Green I Master Plus mix (Roche Diagnostics, Barcelona, Spain). Hexon primer sequences were as follows: forward 5′ GCCGCAGTGGTCTTACATGCACATC 3′ and reverse 5′ CAGCACGCCGCGGATGTCAAAG 3′. The adenovirus copy number was quantified with a standard curve, consisting of adenovirus DNA dilutions (10-10^7 copies) in a background of liver mouse genomic DNA. Samples and standards were amplified in triplicate, and the average number of total copies was normalized to copies per cell based on the input DNA weight amount and a genome size of 6×10^9 bp/cell. Results are expressed as vp/100 cells.

Statistical Analysis

The descriptive statistical analysis was performed on SPSS software (SYSTAT software, Inc, Chicago, IL). Results are expressed as mean ± SEM. A Mann-Whitney nonparametric test was used for the statistical analysis (2-tailed) of *in vitro* and *in vivo* studies. $P < .05$ was taken as the level of significance.

The *in vivo* tumor growth and survival statistical analysis was performed using S-PLUS functions. In line with the experimental design, animal, repeated measures, and site are considered to be nested classification factors. We associated random-effects terms with the animal factor, the day of measurement, and the site of nesting of the animal. Hence, general linear-mixed models were used to estimate the effects of treatment on tumor growth by taking nested and repeated design into account [24]. These models allowed us to analyze the overall effect and the effect of each treatment. The estimation of the coefficients and associated P values was based on restricted maximum likelihood. A plot with residual *versus* fitted values was used to check the assumptions of the model. With these plots, log transformation of the data was used when homoscedasticity was observed. The variance function structure was used to model heteroscedasticity in the day-to-day errors. $P < .05$ (Bonferroni correction) was considered statistically significant after performing multiple comparisons of the treatment groups.

Survival analyses were also performed to analyze time-to-event probability. The survival curves obtained were compared for the different treatments. Animals whose tumor size never achieved the threshold or that were alive at the end of the experiment were included as right censored information. A log-rank test was used to determine the statistical significance of the differences in time-to-event. P.05 was considered statistically significant.

Results

uPAR Promoter Drives Adenoviral Transgene Expression to Pancreatic Cancer In Vitro *and* In Vivo

We analyzed uPAR expression in a panel of pancreatic cancer cell lines, in pancreatic tumors, and in HPDE cells derived from normal ductal epithelium by semiquantitative reverse transcription (RT)–PCR analysis. uPAR expression was weaker in normal ductal HPDE cells when compared with most of the cancer cells (Figure W1*A*). uPAR expression was also detected in the two different tumor models analyzed (Figure W1*B*). To initially test the pancreatic cancer selectivity of the uPAR promoter, reporter studies were undertaken. Results showed that a 450-bp fragment of uPAR promoter was significantly more active in RWP1 pancreatic cancer cells than in nontumoral cells HPDE or NIH3T3 (Figure 1*A*).

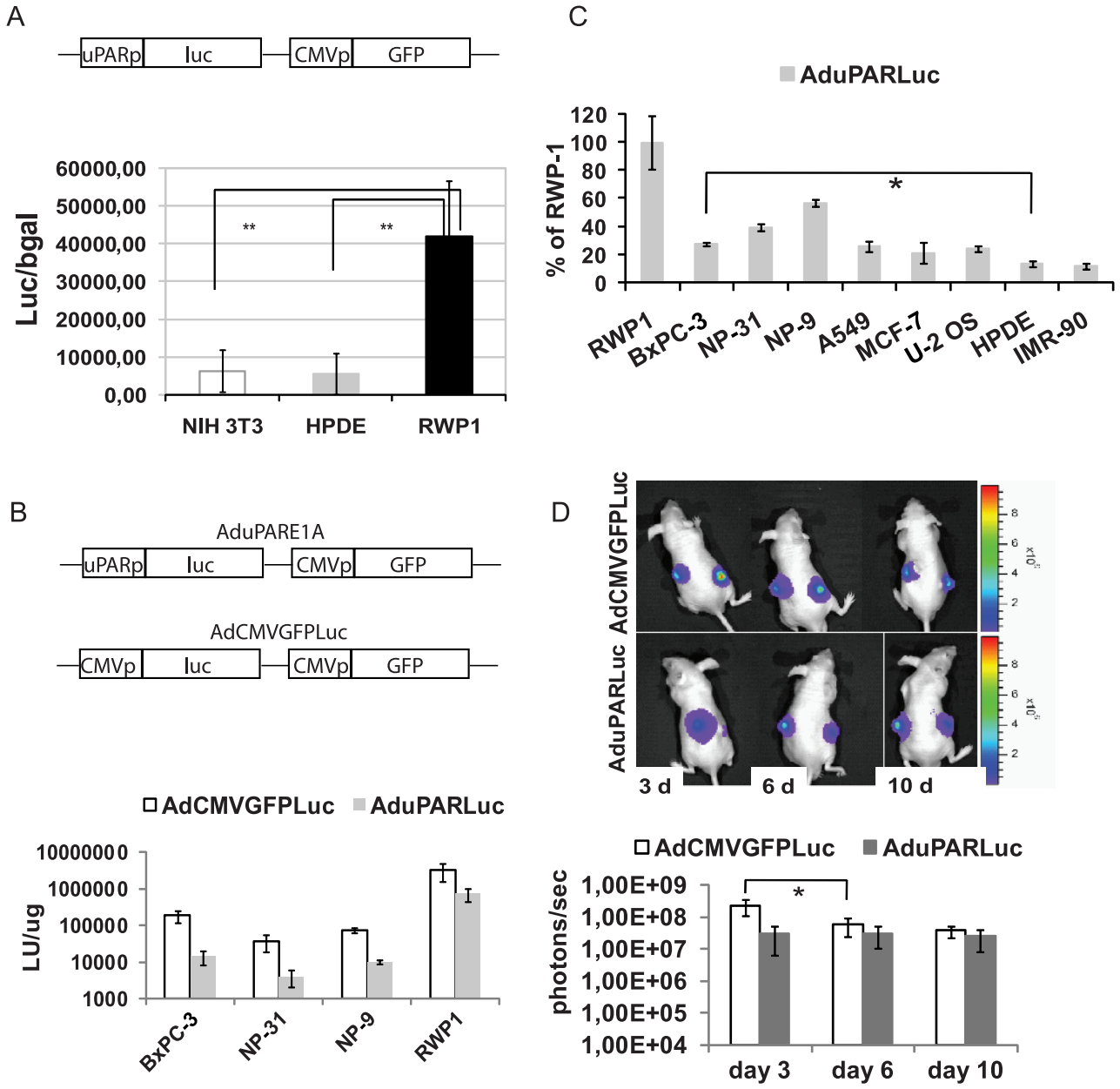

Figure 1. uPAR promoter activity in pancreatic cancer cell lines and in pancreatic tumors. (A) NIH3T3, HPDE, and RWP1 cells were transfected with the plasmid pAdTrackuPARLuc (shown in the scheme). To normalize for transfection efficiency, pCMVβGal plasmid was used. Forty-eight hours later, luciferase and β-galactosidase activities were determined. Results are expressed as light units (LU) relative to β-galactosidase activity and are shown as the mean ± SEM of three independent experiments. $^{**}P = .006$, HPDE *versus* RWP1; $^{**}P = .002$, NIH3T3 *versus* RWP1. (B) A total of 20,000 cells/well were seeded in triplicate and infected with either AduPARLuc or AdCMVGFPLuc at 10^4 vp/cell. Luciferase activity was quantified 72 hours after viral transduction and normalized to total protein levels. Results are expressed as light units per microgram protein. Values are represented as the mean ± SEM of four independent experiments. (C) Percentage of uPAR/CMV luciferase ratio relative to the uPAR/CMV luciferase ratio for RWP1 cells. Values are represented as the mean ± SEM of three or four independent experiments. $^{*}P < .05$. (D) A total of 3×10^6 BxPC-3 cells were injected SC into each posterior flank of nude mice. When tumors achieved a mean volume of 100 mm^3, they were randomized and injected intratumorally with a single 2.5×10^{10} vp dose of AdCMVGFPLuc ($n = 9$) or AduPARLuc ($n = 10$). Shown are representative images and quantification of bioluminescent emission from mice receiving AdCMVGFPLuc (upper panel) or AduPARLuc (lower panel) at days 3, 6, and 10 after viral injection. Results are expressed as photons per second. Values are represented as mean ± SEM. $^{*}P = .03$.

To assess the potential capacity of the uPAR promoter to effectively and selectively target pancreatic cancer, we generated a replication-defective adenovirus, AduPARLuc, which expresses the luciferase reporter gene under the regulation of a 450-bp fragment of the human uPAR promoter (Figure 1*B*). The AdCMVGFPLuc virus, which expresses the luciferase gene under the CMV promoter, was used as a control.

All pancreatic cancer cells infected with the AduPARLuc virus showed high levels of luciferase activity, indicating that the uPAR promoter was active in pancreatic cancer cells. However, when compared with CMV promoter, uPAR promoter activity resulted in 23% to 27% of that of the CMV (Figure 1*B*). Interestingly, the 450-bp fragment of the uPAR promoter had relatively higher luciferase activity in pancreatic

cancer cells and in cells of other cancer origin (lung, breast, and bone) than in the nontumor cells lines HPDE and IMR-90 (Figure 1*C*). This then indicates that the uPAR promoter retains its specificity for cancer cells in the context of an E1A-deleted adenoviral genome.

To identify uPAR activity in pancreatic tumors, BxPC-3 SC xenografts were injected with AduPARLuc or AdCMVGFPLuc at 2.5×10^{10} vp/tumor, and the level and duration of luciferase expression were monitored by optical imaging. Bioluminescence imaging showed that both viruses induced high levels of luciferase expression (Figure 1*D*). In mice receiving the control AdCMVGFPLuc virus, luciferase activity peaked at day 3 but rapidly decreased, showing a significant four-fold reduction in the initial luciferase activity at day 6 after viral injection (Figure 1*D*). By contrast, in AduPARLuc-injected tumors, bioluminescence activity was maintained constant, lasting at least 10 days after viral injection. It is worthy of note that from day 6 to the end of the experiment, both promoters presented similar levels of activity. Similar results were obtained with an NP-18 SC tumor model (data not shown). These findings indicated that uPAR promoter activity in pancreatic tumors is as high as that of the constitutively active CMV promoter (Figure 1*D*).

uPAR Promoter Selectively Targets Pancreatic Cancer Tumors

To address the potential selectivity of the AduPARLuc virus for pancreatic cancer tumors, mice bearing BxPC-3 and PANC-1 xenografts were challenged with a single intravenous (IV) injection of 5×10^{10} vp of the AduPARLuc virus. Luciferase expression was then analyzed in the liver and in the tumors. Data showed that the uPAR promoter activity was as high as that of the CMV in the tumor, whereas a significant reduction in transgene expression was detected in the liver of AduPARLuc-injected animals (Figure 2, *A* and *B*). The cancer-specific index (established as a tumor-to-liver ratio) was significantly higher in AduPARLuc-injected animals in both BxPC-3 (122-fold, $P = .001$) and PANC-1 (23-fold, $P = .006$) SC tumor models (Figure 2, *C* and *D*), indicating that the uPAR promoter was more selective for pancreatic tumor tissue *in vivo*. These results are consistent with the results obtained from the biodistribution studies, where a significantly lower uPAR activity was detected in the liver, spleen, kidneys, heart, and lung, and a very weak activity was observed in the pancreas, intestine, stomach, and testis (Figure W2).

AduPARE1A Induces Significant Cytotoxicity in Pancreatic Cancer Cells

To study whether the uPAR promoter could be a candidate promoter to selectively, efficiently, and safely act against pancreatic cancer, we generated an oncolytic AduPARE1A virus in which the E1A gene expression was regulated by the uPAR promoter. A Kozak sequence was engineered upstream of the E1A gene to increase its replication potency [9]. A DNA fragment from the myotonic dystrophy locus (DM-1), with enhancer-blocking insulator activity, was introduced upstream the uPAR promoter to isolate it from enhancer and transcriptional units from the adenovirus genome [22] (Figure 3*A*).

We tested the cytotoxic effect of AduPARE1A in four pancreatic cancer cell lines and in HPDE cells infected with different doses of AduPARE1A or Adwt. The results showed that the AduPARE1A dose required to cause a 50% reduction in cell viability (ID_{50}) was equivalent

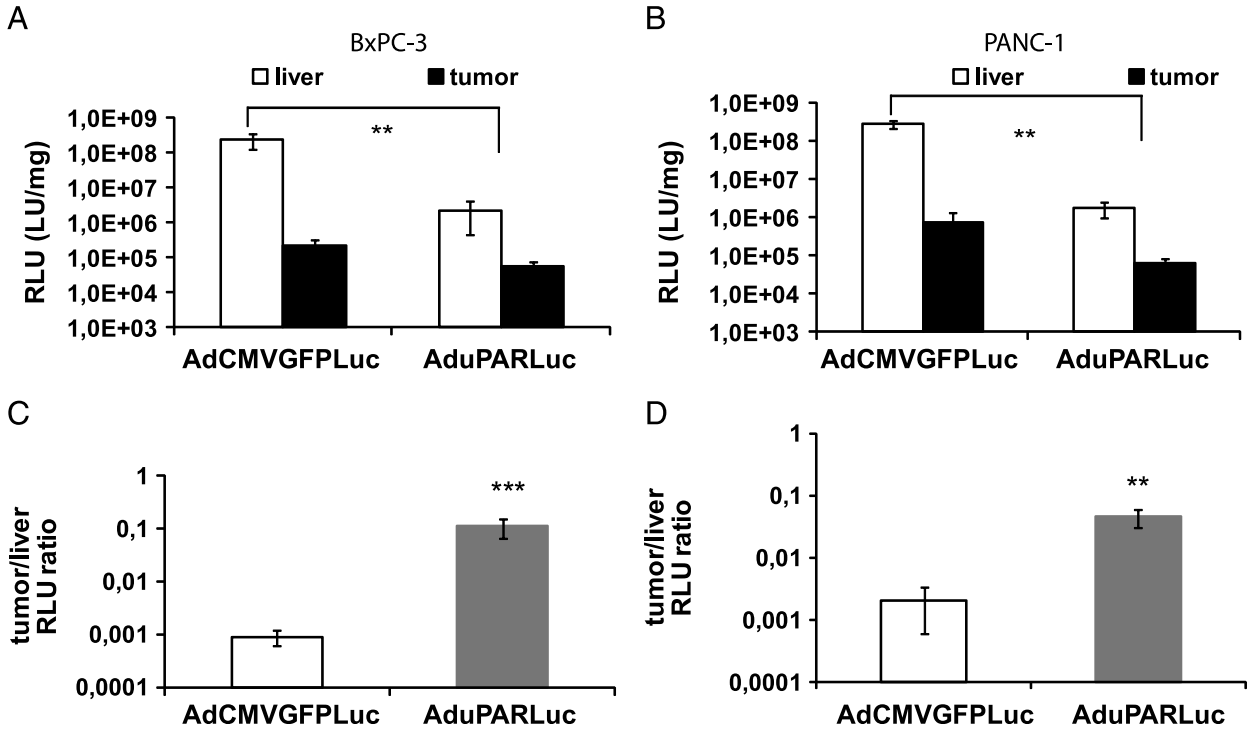

Figure 2. uPAR promoter tumor-to-liver ratio. A total of 3×10^6 BxPC-3 cells (A and C) or 2.5×10^6 PANC-1 cells (B and D) were injected SC into each posterior flank of nude mice. Once tumors were established, animals received 5×10^{10} vp of AdCMVGFPLuc ($n = 4$ mice; $n = 8$ tumors) or AduPARLuc ($n = 4$ mice; $n = 8$ tumors) or saline solution ($n = 2$ mice; $n = 4$ tumors) through the tail vein. Mice were killed 5 days after virus injection, and tumor and liver extracts were assayed for luciferase activity. (A and B) Luciferase activity from liver and tumor tissues. Luciferase activity from the saline group was considered background and subtracted from the viral groups. Results are expressed as light units per milligram of tissue (LU/mg). Values are represented as mean ± SEM. $^{**}P < .01$, $^{***}P < .001$. (C and D) Tumor-to-liver ratio. Values are represented as mean ± SEM of tumor RLU relative to liver RLU. $^{**}P < .01$.

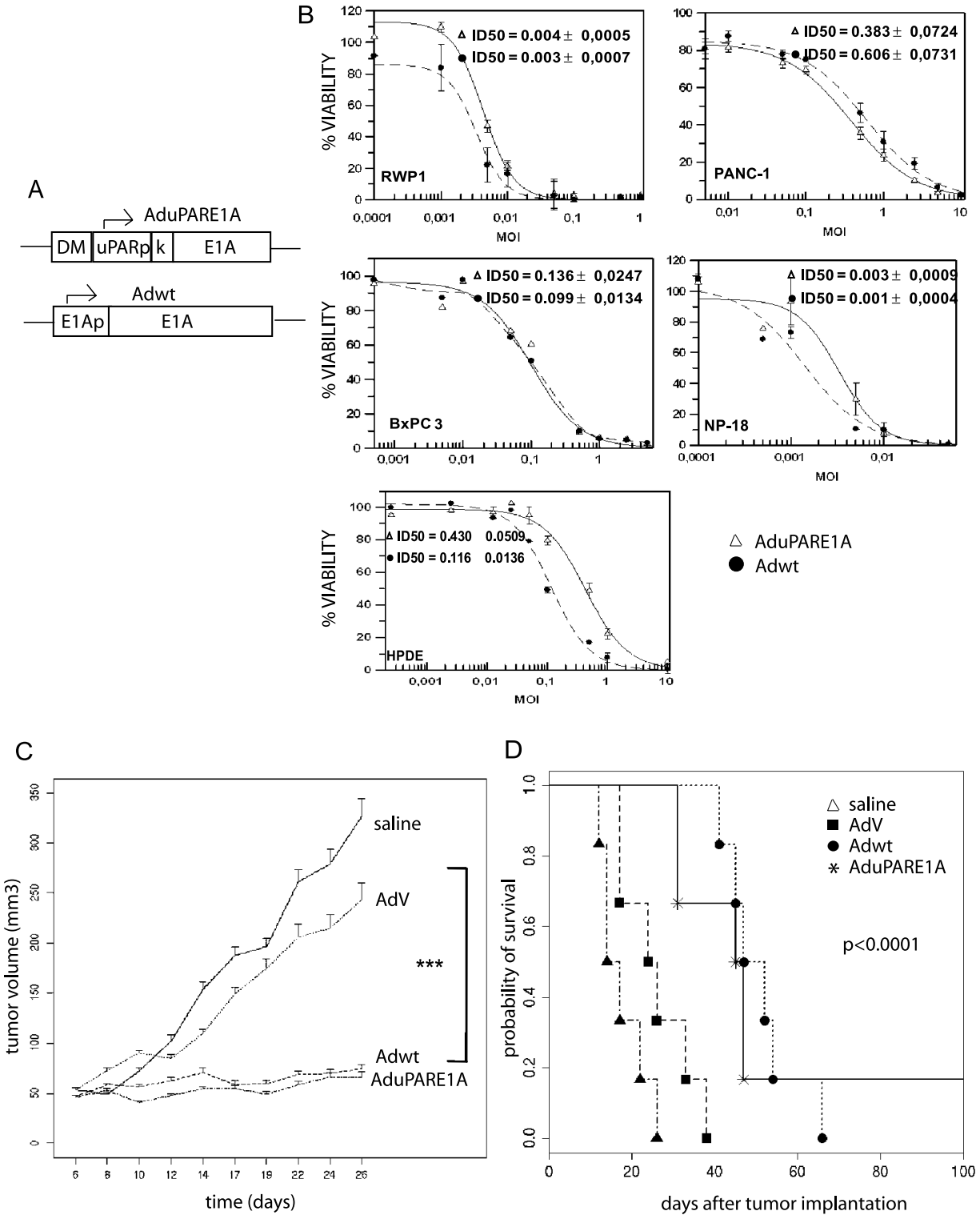

Figure 3. Antitumoral effect of AduPARE1A in pancreatic cancer cells lines, HPDE cells and in BxPC-3 SC xenografts. (A) Schematic representation of the AduPARE1A and Adwt viruses. *DM* indicates myotonic dystrophy fragment; *K*, Kozak sequence. (B) A total of 3×10^3 cells/well were seeded in triplicate and infected with a dose range of 0 to 10 multiplicities of infection of Adwt or AduPARE1A. Cell viability was measured by MTT assay 4 days later and is expressed as the percentage of absorbance of treated wells compared with that of mock-infected cultures. Dose-response curves and ID_{50} values, obtained by a standard nonlinear model based on the Hill equation, are shown as the mean ± SEM of three independent experiments. –●–, Adwt; –△–, AduPARE1A. (C) Animals bearing BxPC-3 SC tumors were randomized to four groups: two control groups, namely, saline ($n = 11$ tumors) and AdV ($n = 11$ tumors), and two treated groups, namely, Adwt ($n = 12$ tumors) and AduPARE1A ($n = 12$ tumors). Animals received intratumoral injections of 10^7 pfu/tumor at days 6 and 14 after tumor implantation. Tumor growth curves are plotted as mean tumor volume ± SEM. ***$P < .0001$. (D) Kaplan-Meier survival curves (log-rank test, <.0001). End point (animals with a tumor volume, ≥300 mm^3).

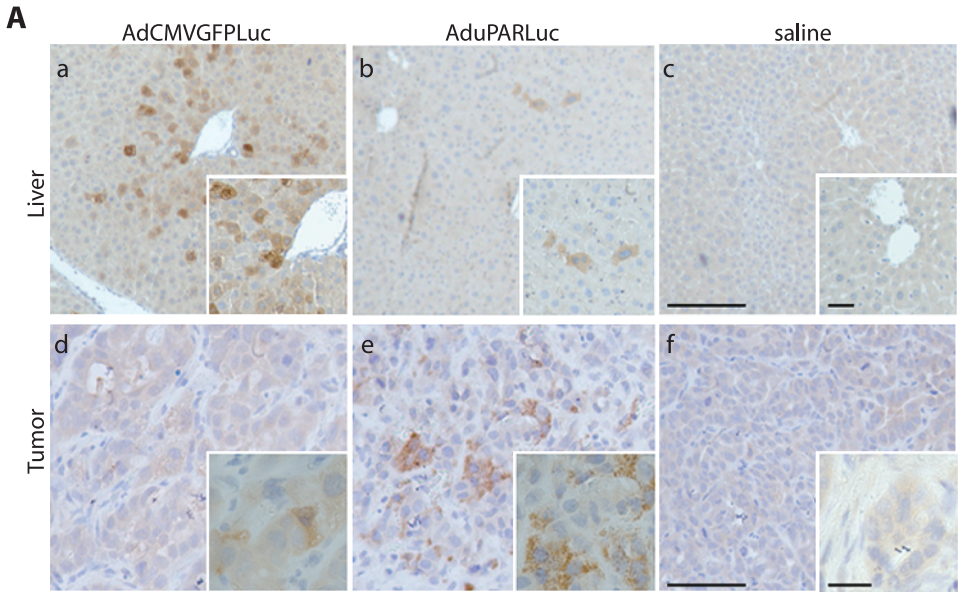

B

	TUMOR POSITIVE CELLS		LIVER POSITIVE CELLS	
group	AdCMVGFPLuc	AduPARLuc	AdCMVGFPLuc	AduPARLuc
(cel./mm2)	4,13 ± 0,65	10,71 ± 0,94	194,28 ± 38,89	32,02 ± 9,38
p value	p=0,05		p=0,001	

Figure 4. AduPARLuc expression in liver metastasis model. Animals bearing PANC-1 tumor metastases received saline solution ($n = 3$) or 5×10^{10} vp of AdCMVGFPLuc ($n = 3$) or AduPARLuc ($n = 3$) IV. Three days later, animals were killed, livers were excised, and luciferase expression was determined by immunohistochemistry with a polyclonal anti–luciferase antibody. (A) Representative images of luciferase expression in liver (a, b, c) and tumor areas (d, e, f) of animals injected with AdCMVGFPLuc or AduPARLuc or saline. (a, b, c) Scale bar, 200 μm; original magnifications, 100 μm. (d, e, f) Scale bar, 50 μm; original magnifications, 20 μm. (B) Stereological analysis. Quantification of luciferase-positive cells in the liver and tumor. Values are shown as the mean ± SEM of three animals. Results are expressed as cells per total area analyzed (cells/mm^2).

to the ID_{50} of the Adwt in the cancer cell lines but was higher for the nontumoral cell line HPDE. These data show that AduPARE1A displays an important cytotoxic effect in pancreatic tumor cells, with a potency similar to that of Adwt (Figure 3*B*). No reduction in cell viability was observed when a nonreplicative empty vector (AdV) was used at similar viral doses (data not shown), demonstrating that the cytotoxic effect observed was specifically due to viral replication and not to nonspecific viral toxicity.

AduPARE1A Represses Tumor Growth and Prolongs Mouse Survival in BxPC-3 SC Xenografts

Next, we evaluated the antitumoral effect of the AduPARE1A oncolytic virus in pancreatic tumors. BxPC-3 SC xenografts received two injections, weekly separated, of 10^7 pfu/tumor of AduPARE1A or Adwt or AdV or saline solution. As shown in Figure 3*C*, a significant reduction in tumoral growth was observed in both treated groups (AduPARE1A and Adwt) compared with the saline or AdV control groups ($P < .0001$). Importantly, 25% (3/12) of AduPARE1A-injected tumors and 16% (2/12) of Adwt-injected tumors were completely eradicated and no tumor burden detected when some of the animals were killed owing to the growth of the contralateral tumor. The median survival time for mice receiving AdV control was 32 days. In contrast, the median survival time for mice receiving AduPARE1A was 51 days ($P < .01$; Figure 3*D*). Moreover, it is worth mentioning that one of the six mice treated with AduPARE1A did not show any tumor burden in either of the two injected tumors 6 months after treatment, indicating that there was no recurrence of the tumors eradicated.

AduPARE1A Represses Tumor Growth and Prolongs Mouse Survival in a Metastasis Tumor Model

The uPAR is a key factor in invasion and metastasis. In this respect, high levels of uPAR expression have been described in human pancreatic cancer metastases [14]; therefore, we hypothesized that the uPAR promoter could also selectively target pancreatic tumor metastasis. To ascertain this, we first established a metastasis model by inoculating PANC-1 cells into the spleen of nude mice (Figure W3). By day 10 of tumor cell inoculation, when metastatic liver nodules were present, mice were injected IV with 5×10^{10} vp of AduPARLuc or AdCMVGFPLuc. Luciferase immunostaining in liver sections revealed strong immunoreactivity in PANC-1 tumor cells in both AduPARLuc- and AdCMVGFPLuc-treated mice (Figure 4*A*). The proportion of luciferase-positive tumor cells in AduPARLuc-treated mice was significantly higher than that in AdCMVGFPLuc mice (Figure 4*B*). Interestingly, in the liver parenchyma, luciferase expression was detected at very low levels and in a limited number of cells in the AduPARLuc-treated mice, whereas strong luciferase staining and a significant increased

proportion of luciferase-positive hepatocytes were detected in the AdCMVGFPLuc group (Figure 4*A*), providing new evidence of the selectivity of the uPAR promoter.

To evaluate the effectiveness of AduPARE1A on the metastatic model, PANC-1 luciferase-expressing cells were inoculated into the spleen of nude mice. Six days later, once the metastases were formed (Figure 5*A*), the animals were treated IV with saline or with a single dose of 10^{10} vp or 5×10^{10} vp of AduPARE1A. Seven days after virus administration, both treated groups presented lower luciferase activity than control animals did. A significant 50% reduction in initial luciferase activity was detected in animals receiving the highest viral dose ($P = .005$; Figure 5*B*). To better address whether this reduction in luciferase-positive cells correlated with a reduction in liver tumors, representative animals from each group were killed at day 21 after treatment. No tumor nodules were found in the liver parenchyma of the 5×10^{10} vp AduPARE1A-treated mice (Figure 5*C*). The number of nodules found was also lower in the animals treated with 10^{10} vp AduPARE1A than in saline-treated mice (data not shown). The median survival time of the saline injected mice

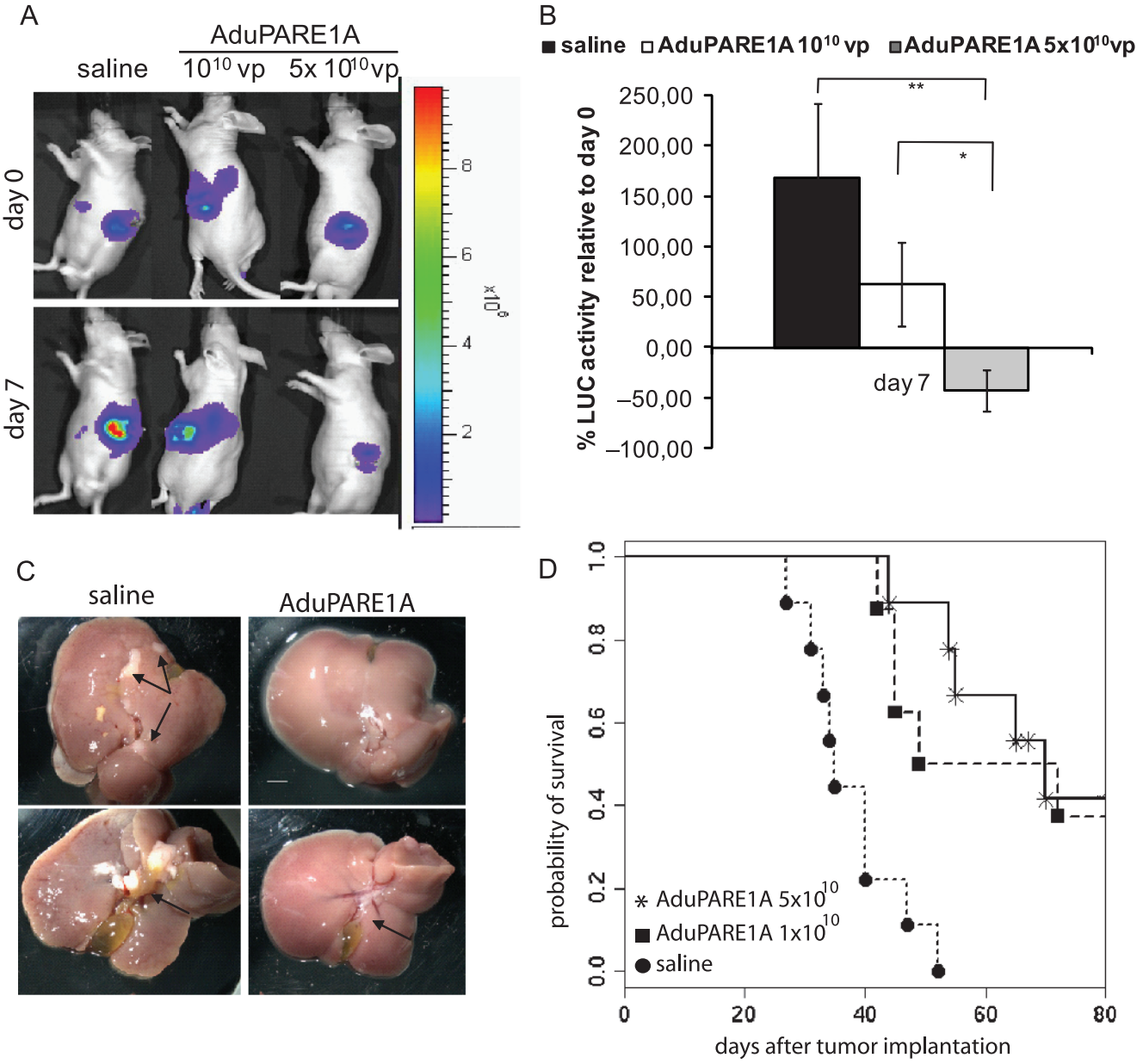

Figure 5. Antitumoral effect of AduPARE1A in PANC-1-Luc liver metastasis model. PANC-1-Luc cells were injected intrasplenically into BALB/c male mice. Six days after tumor implantation bioluminescent activity was recorded (day 0). The day after, animals received a single IV injection, of either saline ($n = 10$) or AduPARE1A at 10^{10} vp/animal ($n = 8$) or AduPARE1A at 5×10^{10} vp/animal ($n = 10$) in a Vf = 0.2 ml. (A) Bioluminescent images of liver metastases-bearing mice at days 0 and 7 after adenoviral treatment. (B) Bioluminescent emission quantification at day 7 relative to day 0. $^{**}P = .005$, $^{*}P = .02$. (C) Representative images of livers excised at day 21 after treatment. Tumor nodules and bile duct obstruction are shown in the saline group (arrows, left panels). Normal bile duct in the 5×10^{10} AduPARE1A–injected animals (arrow, right panels). Scale bar, 1.7 cm. (D) Kaplan-Meier survival curves. AduPARE1A 10^{10} vp *versus* saline log-rank test = .003; AduPARE1A 5×10^{10} vp *versus* saline log-rank test = 5.43×10^{-5}. End point (decreased body weight ≥20% or animal experiencing jaundice).

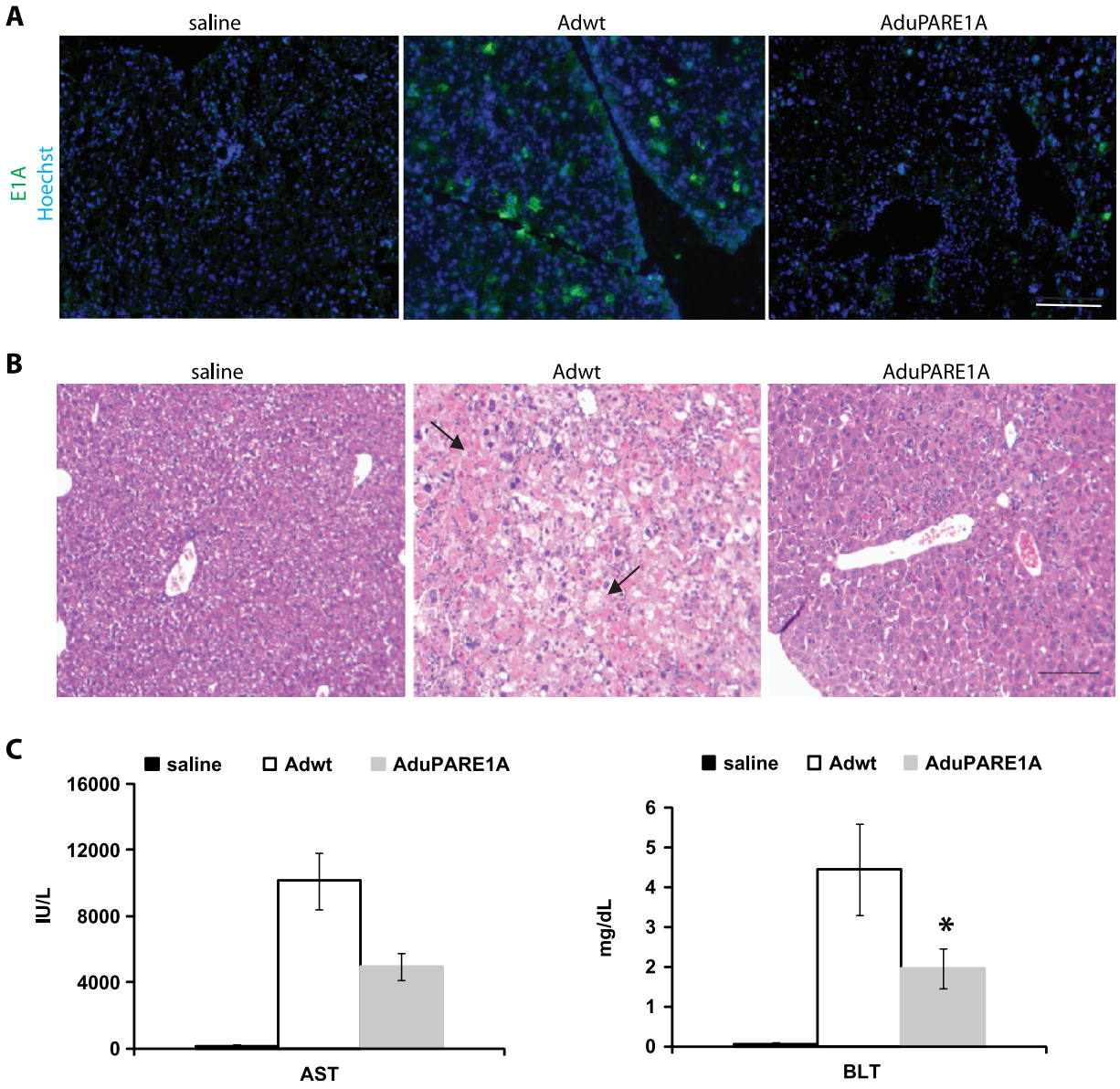

Figure 6. AduPARE1A toxicity studies. BALB/c immunocompetent mice received IV saline solution ($n = 6$) or 5×10^{10} vp of Adwt ($n = 6$) or 5×10^{10} vp of AduPARE1A ($n = 6$). Five days later, blood samples were collected. Next, animals were killed, and the liver tissue excised was frozen in OCT or fixed and embedded in paraffin. (A) E1A expression in the liver tissue. Nuclei were stained with Hoechst. Scale bar, 100 μm. (B) Hematoxylin and eosin staining of liver tissue. Necrotic and swollen hepatocytes (arrows). Scale bar, 1.3 cm. (C) AST and BLT determination. *$P < .05$.

was 35 days, whereas the median survival time of both treated groups was significantly longer, that is, 60 days for the 10^{10} vp viral dose and 70 days for the 5×10^{10} vp dose (Figure 5*D*). Surviving mice (33%) were alive for more than 5 months with no symptoms of morbidity. Then, they were killed and no tumors were observed in any abdominal organ indicating tumor eradication.

uPAR Promoter Presents Low Liver Toxicity on IV Injection

After intravascular injection, adenoviruses liver tropism leads to liver toxicity, caused by an immune response to the viral proteins as well as transgene expression.

First, we evaluated the potential toxicity of AduPARLuc after IV injection in immunocompetent mice and compared it to that of AdCMVGFPLuc. Minimal liver histopathologic changes were observed in AduPARLuc animals in contrast to the hepatocytotoxicity found in all AdCMVGFPLuc liver sections. Importantly, all animals that received the AduPARLuc virus presented AST levels within the reference range (Figure W4). To discard differences in liver viral transduction between the AduPARLuc- and AdCMVGFPLuc-injected mice, we assessed the amount of viral particles in the liver by quantitative real-time PCR. Quantification showed a similar amount of viral particles in both groups (AdCMVGFPLuc 13.14 ± 1.33 vp/100 cells and AduPARLuc 10.82 ± 0.92 vp/100 cells) indicating that the toxicity elicited by transgene expression in the liver, in the context of a replication-defective adenovirus, can be minimized by the uPAR promoter.

Next, we studied the potential liver toxicity of the oncolytic AduPARE1A and compared it to that of Adwt. E1A Immunostaining revealed negligible E1A expression in the liver sections of AduPARE1A-injected animals, whereas strong immunoreactivity was detected in the liver of Adwt mice (Figure 6*A*). Consistently, lower areas of

hepatocyte swelling and necrotic hepatocytes were observed in the liver sections of AduPARE1A-injected mice compared with Adwt-injected mice (Figure 6*B*). Moreover, serum levels of AST and BLT were significantly lower in AduPARE1A-injected mice than those in Adwt-injected mice (Figure 6*C*). Furthermore, a 50% mortality rate was detected in the 5×10^{10} vp Adwt-injected animals, whereas all the animals injected with this dose of AduPARE1A survived. The data thus indicate that the uPAR promoter provided reduced toxicity to the replication-competent AduPARE1A virus.

Discussion

Oncolytic virotherapy is a promising approach for the systemic treatment of cancers, such as pancreatic cancer, characterized by the rapid dissemination of the tumor and the lack of any effective treatment. However, the need of highly selective and efficient viruses is a requisite for a safe and significant therapeutic benefit. Transcriptional targeting strategies based on using TSP to redirect adenoviral gene expression and replication have proved the importance of such approaches to achieve tumor specificity. uPAR expression has been shown to be transcriptionally upregulated in pancreatic ductal adenocarcinoma, compared with normal pancreatic cells, suggesting that the factors driving uPAR transcription may be highly active in a tumoral context. In this study, we have demonstrated that the uPAR promoter in an adenovirus vector delivers potent activity in all the pancreatic cancer cell lines studied, although lower than that of the CMV promoter (10%-22% of the latter). Interestingly, such differences were no longer found on intratumoral or intravascular viral administration in mice bearing pancreatic SC xenografts. Thus, *in vivo*, the uPAR promoter activity in the tumors was similar to that of the CMV promoter, suggesting that in the tumor either CMV promoter activity is reduced or uPAR promoter activity is favored. Most probably, both phenomena take place. In fact, a comparative analysis of uPAR and CMV promoter activity *in vivo* showed persistent luciferase expression in the AduPARLuc-injected tumors, in contrast to a significant decrease in luciferase expression 1 week after AdCMVGFPLuc injection. This effect could be related to the susceptible epigenetic inactivation of robust but exogenous promoters such as CMV, whereas such effects may be less relevant when using endogenous promoters [25]. On the other hand, one could hypothesize that tumor environment factors could positively regulate uPAR expression. In line with this, a lower oxygen pressure within the tumor environment has been described to positively regulate uPAR expression in several types of tumor [26]. Furthermore, uPAR has been found to be upregulated in the tumor stroma [27] and in the invasive front of pancreatic tumors [28].

Significant uPAR tumoral activity would be in line with the remarkable antitumor response achieved with the intratumoral administration of the conditionally replicating adenovirus AduPARE1A, which completely eradicates 25% of the BxPC-3 SC–treated tumors and offers a significant increase in survival rates. The significant response achieved might also be accounted for additional mechanisms, such as the fact that the AduPARE1A virus demonstrated a strong *in vitro* cytocidal effect, similar to that of Adwt. Such similar *in vitro* potency is highly relevant because a loss of potency has been reported with some oncolytic adenoviruses that use TSP. The introduction of a Kozak sequence in the *E1A* gene may have facilitated E1A translation. Indeed, it has been proposed that achieving near wild-type levels of E1A could be required to maintain efficient adenoviral replication [29].

One of the major challenges was to demonstrate cancer selectivity of the uPAR promoter for pancreatic cancer and metastasis. The first evidence emerged from the *in vitro* data, which showed that uPAR activity was significantly higher in pancreatic cancer cells than in normal pancreatic or embryonic lung cells. Notably, the cancer-specific index of the uPAR promoter was significantly higher than that of CMV, as shown by the 2-log increase in the tumor-to-liver ratio. In this respect, biodistribution studies of tumor-free mice confirmed that uPAR promoter activity was very weak in normal tissue. This is not surprising because uPAR expression in the normal tissue of adult mice has been reported to be restricted to the placenta and epididymis [30]. More importantly, our results demonstrate that upon intravascular delivery, uPAR promoter activity is significantly higher than that of the CMV promoter in tumor metastases in the liver, resulting in a significant increase in tumor selectivity. Accordingly, AduPARE1A shows a potent antitumoral effect in metastasis bearing mice, resulting in a significant reduction of tumor burden at day 7, eradication of metastasis in 33% of mice, and a significant increase in survival rates. The specificity of the uPAR promoter was further demonstrated by the systemic toxicity studies of immunocompetent mice. It is worth mentioning that, at the highest therapeutic viral dose used (5×10^{10}), whereas a 50% mortality rate was recorded for Adwt, as previously reported [9], all the animals receiving the AduPARE1A virus survived the course of the study, indicating that AduPARE1A presents a wider therapeutic window.

The uPAR promoter could also be potentially suited to targeting other types of cancer, as shown by increased uPAR activity in breast and lung cancer cell lines, compared with normal cells. Along such lines, uPAR has been found to be overexpressed in several types of cancer, such as breast [18], prostate [31], and colon cancer [32]. Moreover, the 0.4-kb uPAR promoter used in this study is positively regulated by the Sp1 transcription factor [17], which has been shown to activate the uPAR promoter in colon cancer [32], suggesting the ubiquitous cancer-specific activity of the uPAR promoter.

Altogether, our results indicate that we have developed a potent IV-administered therapeutic agent, capable of great activity and selectivity for pancreatic tumor tissue, yet with low toxicity in normal tissue. Thus, AduPARE1A is a promising therapeutic agent for the treatment of pancreatic cancer and has the potential to be effective in other types of cancer. Future studies on arming this therapeutic virus with candidate transgenes may lead to further enhancing its antitumoral activity.

Acknowledgments

The authors thank Núria Andreu and Meritxell Carrió for technical assistance. The authors thank Francesco Blasi for providing the plasmid pCAT-Basic-uPAR(C2).

References

[1] Rustgi AK (2006). The molecular pathogenesis of pancreatic cancer: clarifying a complex circuitry. *Genes Dev* **20**, 3049–3053.

[2] Saif MW (2007). Pancreatic cancer: are we moving forward yet? Highlights from the Gastrointestinal Cancers Symposium. Orlando, FL, USA. January 20th, 2007. *JOP* **8**, 166–176.

[3] Alemany R (2007). Cancer selective adenoviruses. *Mol Aspects Med* **28**, 42–58.

[4] Nemunaitis J, Senzer N, Sarmiento S, Zhang YA, Arzaga R, Sands B, Maples P, and Tong AW (2007). A phase I trial of intravenous infusion of ONYX-015 and enbrel in solid tumor patients. *Cancer Gene Ther* **14**, 885–893.

[5] Hecht JR, Bedford R, Abbruzzese JL, Lahoti S, Reid TR, Soetikno RM, Kirn DH, and Freeman SM (2003). A phase I/II trial of intratumoral endoscopic ultrasound injection of ONYX-015 with intravenous gemcitabine in unresectable pancreatic carcinoma. *Clin Cancer Res* **9**, 555–561.

[6] Ohashi M, Kanai F, Tanaka T, Lan KH, Shiratori Y, Komatsu Y, Kawabe T, Yoshida H, Hamada H, and Omata M (1998). *In vivo* adenovirus-mediated prodrug gene therapy for carcinoembryonic antigen–producing pancreatic cancer. *Jpn J Cancer Res* **89**, 457–462.

[7] Wesseling JG, Yamamoto M, Adachi Y, Bosma PJ, van Wijland M, Blackwell JL, Li H, Reynolds PN, Dmitriev I, Vickers SM, et al. (2001). Midkine and cyclooxygenase-2 promoters are promising for adenoviral vector gene delivery of pancreatic carcinoma. *Cancer Gene Ther* **8**, 990–996.

[8] Xie X, Xia W, Li Z, Kuo HP, Liu Y, Ding Q, Zhang S, Spohn B, Yang Y, Wei Y, et al. (2007). Targeted expression of BikDD eradicates pancreatic tumors in noninvasive imaging models. *Cancer Cell* **12**, 52–65.

[9] Cascallo M, Alonso MM, Rojas JJ, Perez-Gimenez A, Fueyo J, and Alemany R (2007). Systemic toxicity-efficacy profile of ICOVIR-5, a potent and selective oncolytic adenovirus based on the pRB pathway. *Mol Ther* **15**, 1607–1615.

[10] Ramirez PJ, Vickers SM, Ono HA, Davydova J, Takayama K, Thompson TC, Curiel DT, Bland KI, and Yamamoto M (2008). Optimization of conditionally replicative adenovirus for pancreatic cancer and its evaluation in an orthotopic murine xenograft model. *Am J Surg* **195**, 481–490.

[11] Yamamoto M, Davydova J, Wang M, Siegal GP, Krasnykh V, Vickers SM, and Curiel DT (2003). Infectivity enhanced, cyclooxygenase-2 promoter–based conditionally replicative adenovirus for pancreatic cancer. *Gastroenterology* **125**, 1203–1218.

[12] Blasi F and Carmeliet P (2002). uPAR: a versatile signalling orchestrator. *Nat Rev Mol Cell Biol* **3**, 932–943.

[13] Han H, Bearss DJ, Browne LW, Calaluce R, Nagle RB, and Von Hoff DD (2002). Identification of differentially expressed genes in pancreatic cancer cells using cDNA microarray. *Cancer Res* **62**, 2890–2896.

[14] Sawai H, Okada Y, Funahashi H, Matsuo Y, Takahashi H, Takeyama H, and Manabe T (2006). Interleukin-1alpha enhances the aggressive behavior of pancreatic cancer cells by regulating the alpha6beta1-integrin and urokinase plasminogen activator receptor expression. *BMC Cell Biol* **7**, 8.

[15] Pillay V, Dass CR, and Choong PF (2007). The urokinase plasminogen activator receptor as a gene therapy target for cancer. *Trends Biotechnol* **25**, 33–39.

[16] Bauer TW, Liu W, Fan F, Camp ER, Yang A, Somcio RJ, Bucana CD, Callahan J, Parry GC, Evans DB, et al. (2005). Targeting of urokinase plasminogen activator receptor in human pancreatic carcinoma cells inhibits c-Met- and insulin-like growth factor-I receptor–mediated migration and invasion and orthotopic tumor growth in mice. *Cancer Res* **65**, 7775–7781.

[17] Soravia E, Grebe A, De Luca P, Helin K, Suh TT, Degen JL, and Blasi F (1995). A conserved TATA-less proximal promoter drives basal transcription from the urokinase-type plasminogen activator receptor gene. *Blood* **86**, 624–635.

[18] Carrio M, Arderiu G, Myers C, and Boudreau NJ (2005). Homeobox D10 induces phenotypic reversion of breast tumor cells in a three-dimensional culture model. *Cancer Res* **65**, 7177–7185.

[19] Bayo-Puxan N, Cascallo M, Gros A, Huch M, Fillat C, and Alemany R (2006). Role of the putative heparan sulfate glycosaminoglycan-binding site of the adenovirus type 5 fiber shaft on liver detargeting and knob-mediated retargeting. *J Gen Virol* **87**, 2487–2495.

[20] Liu N, Furukawa T, Kobari M, and Tsao MS (1998). Comparative phenotypic studies of duct epithelial cell lines derived from normal human pancreas and pancreatic carcinoma. *Am J Pathol* **153**, 263–269.

[21] Alemany R and Curiel DT (2001). CAR-binding ablation does not change biodistribution and toxicity of adenoviral vectors. *Gene Ther* **8**, 1347–1353.

[22] Majem M, Cascallo M, Bayo-Puxan N, Mesia R, Germa JR, and Alemany R (2006). Control of E1A under an E2F-1 promoter insulated with the myotonic dystrophy locus insulator reduces the toxicity of oncolytic adenovirus Ad-Delta24-RGD. *Cancer Gene Ther* **13**, 696–705.

[23] Huch M, Abate-Daga D, Roig JM, Gonzalez JR, Fabregat J, Sosnowski B, Mazo A, and Fillat C (2006). Targeting the CYP2B1/cyclophosphamide suicide system to fibroblast growth factor receptors results in a potent antitumoral response in pancreatic cancer: models. *Hum Gene Ther* **17**, 1187–1200.

[24] Heitjan DF, Manni A, and Santen RJ (1993). Statistical analysis of *in vivo* tumor growth experiments. *Cancer Res* **53**, 6042–6050.

[25] Brooks AR, Harkins RN, Wang P, Qian HS, Liu P, and Rubanyi GM (2004). Transcriptional silencing is associated with extensive methylation of the CMV promoter following adenoviral gene delivery to muscle. *J Gene Med* **6**, 395–404.

[26] Trisciuoglio D, Iervolino A, Candiloro A, Fibbi G, Fanciulli M, Zangemeister-Wittke U, Zupi G, and Del Bufalo D (2004). bcl-2 induction of urokinase plasminogen activator receptor expression in human cancer cells through Sp1 activation: involvement of ERK1/ERK2 activity. *J Biol Chem* **279**, 6737–6745.

[27] Giannopoulou I, Mylona E, Kapranou A, Mavrommatis J, Markaki S, Zoumbouli C, Keramopoulos A, and Nakopoulou L (2007). The prognostic value of the topographic distribution of uPAR expression in invasive breast carcinomas. *Cancer Lett* **246**, 262–267.

[28] Tan X, Egami H, Nozawa F, Abe M, and Baba H (2006). Analysis of the invasion-metastasis mechanism in pancreatic cancer: involvement of plasmin(ogen) cascade proteins in the invasion of pancreatic cancer cells. *Int J Oncol* **28**, 369–374.

[29] Nettelbeck DM, Rivera AA, Balague C, Alemany R, and Curiel DT (2002). Novel oncolytic adenoviruses targeted to melanoma: specific viral replication and cytolysis by expression of E1A mutants from the tyrosinase enhancer/promoter. *Cancer Res* **62**, 4663–4670.

[30] Wang H, Hicks J, Khanbolooki P, Kim SJ, Yan C, Wang Y, and Boyd D (2003). Transgenic mice demonstrate novel promoter regions for tissue-specific expression of the urokinase receptor gene. *Am J Pathol* **163**, 453–464.

[31] Gavrilov D, Kenzior O, Evans M, Calaluce R, and Folk WR (2001). Expression of urokinase plasminogen activator and receptor in conjunction with the ets family and AP-1 complex transcription factors in high grade prostate cancers. *Eur J Cancer* **37**, 1033–1040.

[32] Allgayer H, Wang H, Gallick GE, Crabtree A, Mazar A, Jones T, Kraker AJ, and Boyd DD (1999). Transcriptional induction of the urokinase receptor gene by a constitutively active Src. Requirement of an upstream motif (–152/–135) bound with Sp1. *J Biol Chem* **274**, 18428–18437.

Supplemental Data

uPAR Messenger RNA Determination

RNA was extracted from semiconfluent cell cultures, from BxPC-3 xenografts, and from PANC-1 liver metastases using the RNeasy Mini RNA Extraction Kit (Qiagen). One microgram of total RNA was reverse-transcribed using Moloney Murine Leukemia Virus reverse transcriptase (Ambion, Austin, TX) and 1/10 of this reaction was linearly amplified for 23 cycles (cell lines) or 28 cycles (tumor samples) after denaturation (30 seconds at 95°C), annealing (30 seconds at 60°C), and extension (30 seconds at 72°C) in a thermal cycler (GeneAmp PCR System 9700; Applied Biosystems, London, UK). The following primers were used: forward 5′ CAGGACCTCTGCAGGACCAC 3′, reverse 5′ CCTTGCAGCTGTAACACTGG 3′. Total RNA was normalized using QuantumRNA 18S Internal Standards at a 1:4 ratio (Ambion).

Biodistribution Studies

BALB/c nude male mice (Charles River France, Lyon, France) received 2×10^{10} vp of AdCMVGFPLuc or AduPARLuc or saline solution through tail vein injection in a final volume of 200 µl. At days 3, 5, 11, 20, 31 and 50 after adenoviral transduction, luciferase activity was visualized and quantified using an *in vivo* bioluminescent imaging system (IVIS; Xenogen). At day 50, immediately after imaging, mice were killed and organs were removed and frozen. When stated, frozen tissues were mechanically homogenized, 100 mg was used for protein extraction using the Cell Culture Lysis Reagent (Promega) for 15 minutes at 25°C, and 10 µl was assayed for luciferase activity.

Metastasis Model by Intrasplenic Injection of Tumor Cells

Metastatic pancreatic adenocarcinoma animal models were generated following the protocol previously described [1]. Briefly, BALB/c nude mice were anesthetized with isoflurane and placed in the right lateral decubitus. Thereafter, a left subcostal 1-cm incision was made, and 4×10^6 PANC-1 or PANC-1-Luc cells in 50-µl saline solution were injected into the spleen with a 29-G needle. To maintain hemostasis and prevent leakage of tumor cells outside the splenic capsule, a cotton-tipped applicator was applied to the puncture site. After surgery, mice were monitored daily for health and survival.

References

[1] Tseng JF, Farnebo FA, Kisker O, Becker CM, Kuo CJ, Folkman J, and Mulligan RC (2002). Adenovirus-mediated delivery of a soluble form of the VEGF receptor Flk1 delays the growth of murine and human pancreatic adenocarcinoma in mice. *Surgery* **132**, 857–865.

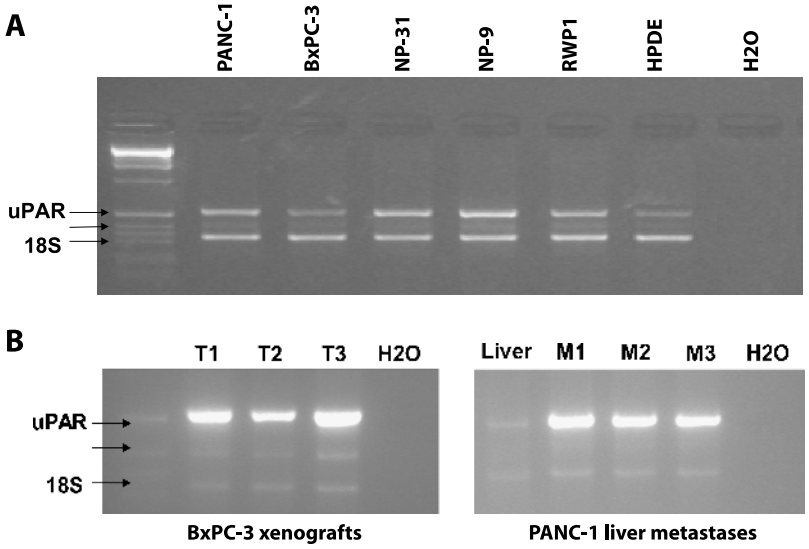

Figure W1. uPAR expression in pancreatic cancer cells, normal cells and tumors. We have analyzed, by semiquantitative RT-PCR analysis, the uPAR expression in five pancreatic cancer cell lines and in normal pancreatic ductal epithelium cell HPDE (A) and in two tumor models (B). Two different transcripts were detected corresponding to the entire form (534-bp fragment) or to one variant lacking one of the L6/uPAR/α-neurotoxin domains of the receptor (400-bp fragment).

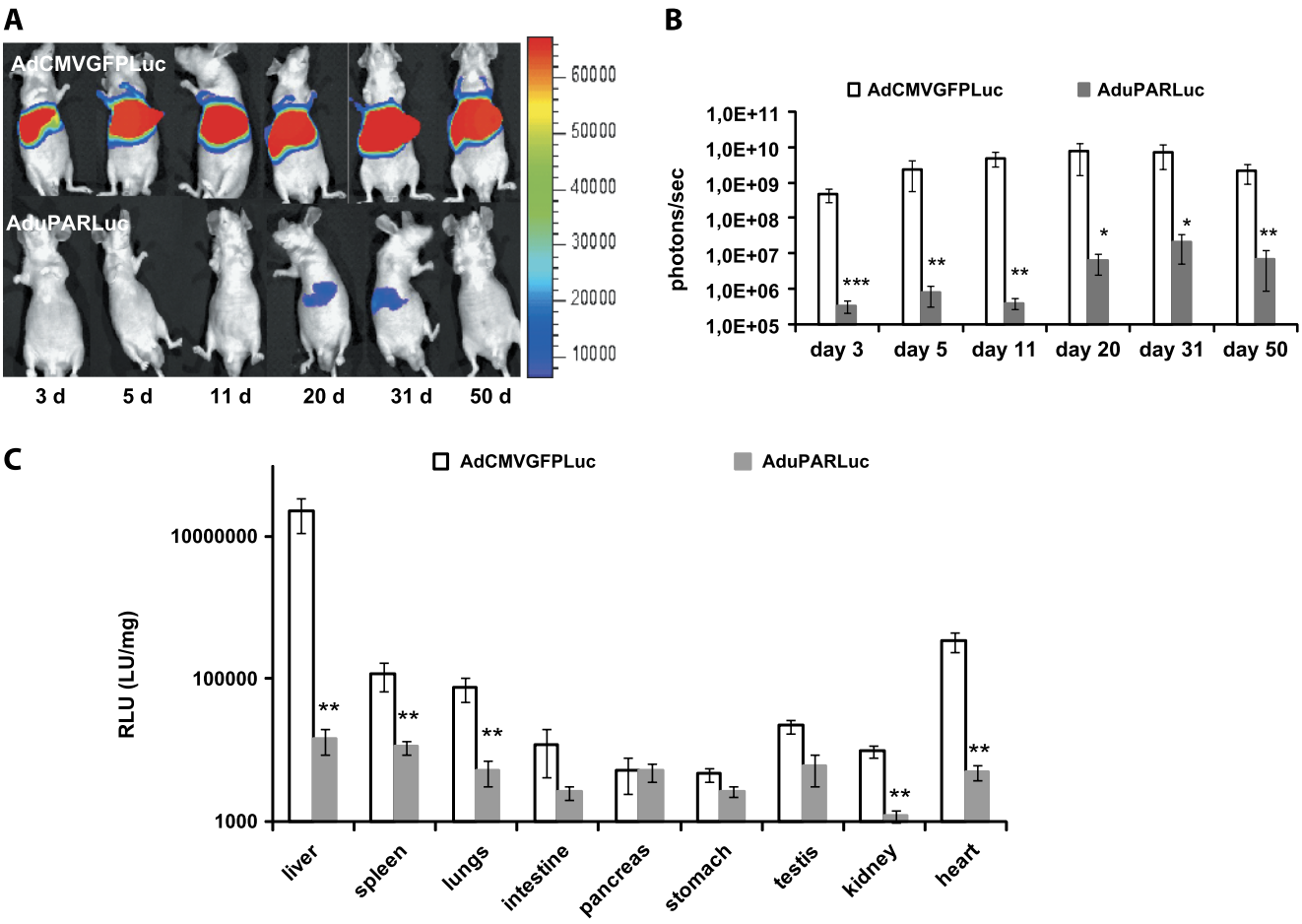

Figure W2. AduPARLuc biodistribution studies. BALB/c nude mice were injected IV with either saline solution ($n = 3$) or 2×10^{10} vp of AdCMVGFPLuc ($n = 4$) or 2×10^{10} vp of AduPARLuc ($n = 5$). Bioluminescent activity was measured in anesthetized animals at days 3, 5, 11, 20, 31, and 50 after viral injection. (A) Representative images of bioluminescent emission. (B) Quantification of bioluminescence emission was performed by measuring the total amount of emitted light captured by the camera. Results are expressed as photons per second. Values are represented as mean ± SEM. ***$P < .001$, **$P < .01$, *$P < .05$. (C) At day 50, animals were killed and organs were collected. Luciferase activity from tissue extracts was determined and normalized to total protein. Luciferase activity from the saline group was considered as the background and subtracted from the viral groups. Results are expressed as light units per milligram of tissue (LU/mg). Values are represented as mean ± SEM. **$P < .01$.

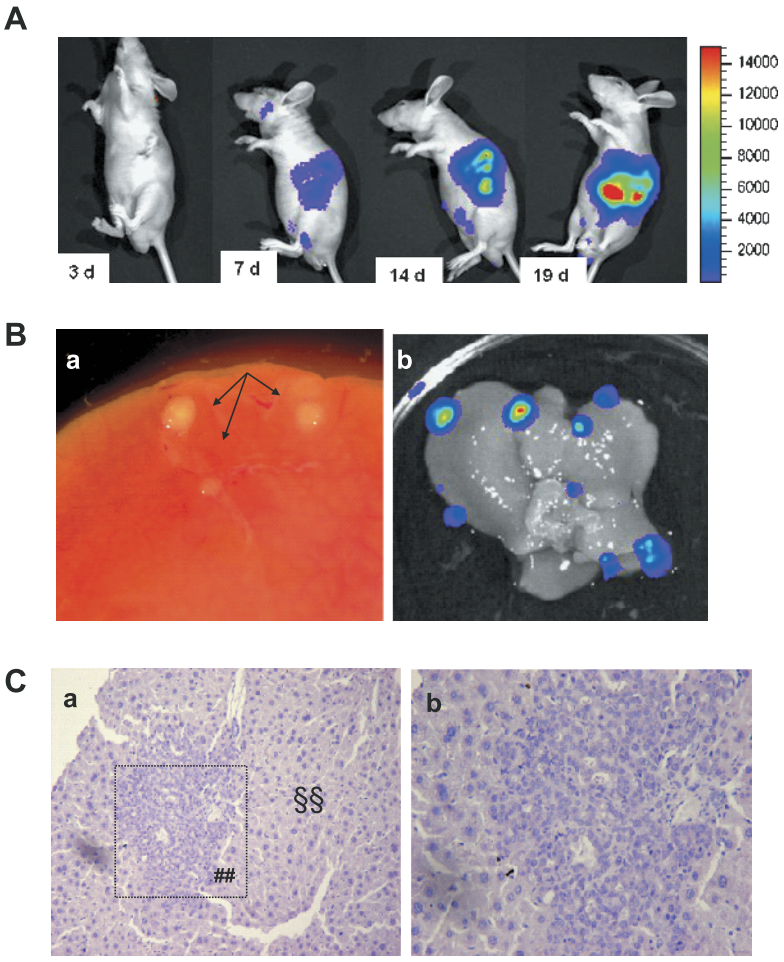

Figure W3. Liver metastases model. Liver metastases were generated by intrasplenic injection of PANC-1-Luc cells into BALB/c nude mice. Luciferase activity was monitored in live animals. At day 19 after tumor implantation, after bioluminescent acquisition, animals were killed, and liver was collected and analyzed for luciferase expression and metastases formation. (A) Representative images of liver. (a) Light image. Original magnification, ×0.8. (b) Bioluminescent image. (B) Histologic analysis of liver tissue by hematoxylin and eosin staining. (a) [§§]Liver area, [##]tumoral area. Original magnification, ×10. (b) Original magnification, ×20.

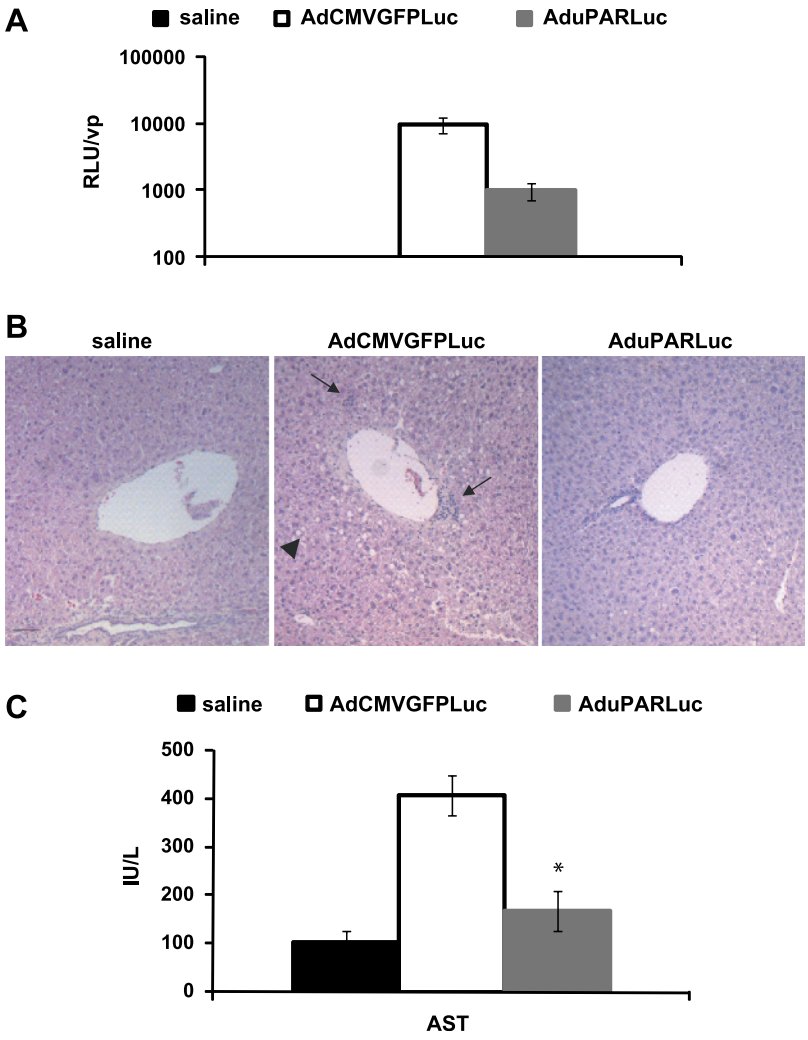

Figure W4. AduPARLuc toxicity studies. BALB/c mice were injected through the tail vein with either saline solution ($n = 4$) or 2×10^{10} vp of AdCMVGFPLuc ($n = 4$) or 2×10^{10} vp of AduPARLuc ($n = 4$). Five days later, blood samples were collected. Next, animals were killed, and the liver tissue was excised. Liver portions were either frozen for luciferase or viral DNA determination, or fixed and embedded in paraffin. (A) Luciferase activity from the liver extracts. Results were normalized to the number of viral particles per milligram of tissue determined by real-time PCR. Results are expressed as light units per milligram (RLU) relative to the number of viral particles (RLU/vp). Values are shown as mean ± SEM. (B) Hematoxylin and eosin staining of liver tissue. Lymphocyte infiltrates (arrows) and necrotic hepatocytes (arrowhead) were only detected in the AdCMVGFPLuc-injected mice. Scale bar, 0.5 mm. (C) AST determination. AST values expressed as international units (IU) per liter. *$P = .02$.